Continuous Flattening of Orthogonal Polyhedra

Erik D. Demaine[1*], Martin L. Demaine[1*], Jin-ichi Itoh[2**], and Chie Nara[3***]

[1] MIT Computer Science and Artificial Intelligence Laboratory, 32 Vassar St., Cambridge, MA 02139,USA, {edemaine,mdemaine}@mit.edu
[2] Faculty of Education, Kumamoto University, Kumamoto, 860-8555, Japan,j-itoh@kumamoto-u.ac.jp
[3] Meiji Institute for Advanced Study of Mathematical Sciences, Meiji University, Nakano, Tokyo 164-8525, Japan, cnara@jeans.ocn.ne.jp

Abstract. Can we flatten the surface of any 3-dimensional polyhedron P without cutting or stretching? Such continuous flat folding motions are known when P is convex, but the question remains open for nonconvex polyhedra. In this paper, we give a continuous flat folding motion when the polyhedron P is an orthogonal polyhedron, i.e., when every face is orthogonal to a coordinate axis (x, y, or z). More generally, we demonstrate a continuous flat folding motion for any polyhedron whose faces are orthogonal to the z axis or the xy plane.

Keywords: folding, continuous flattening, orthogonal polyhedra

1 Introduction

We routinely crush polyhedral boxes to lie flat, but is this possible mathematically? It is known that every polyhedron has a multilayered flat folded state, meaning that it can be *instantaneously* folded to lie in a (multilayer) plane [2, 6]. But is there a continuous motion that does not stretch or rip the material?

In 2001, E. Demaine, M. Demaine, and A. Lubiw [5, 6, 1] asked whether there is a continuous motion of the surface of a polyhedron down to a multilayered flat folded state. For example, J.-i. Itoh and C. Nara [7] showed that the box in Fig. 1(a) continuously folds flat by pushing four side faces in, where the shapes of those four faces are changed continuously by infinitely many creases showed by dashed line segments in Fig. 1(b) and the box reaches the multilayered flat folded state in Fig. 1(c).

An important limitation to continuous flattening is the Bellows Theorem [4]: the volume of any polyhedron with rigid faces is invariant even if it can flex at finitely many additional edges. Flattening a polyhedron necessarily changes the

* Supported in part by NSF ODISSEI grant EFRI-1240383 and NSF Expedition grant CCF-1138967.

** Supported by Grant-in-Aid for Scientific Research(B)(15KT0020) and Scientific Research(C)(26400072).

*** Supported by Grant-in-Aid for Scientific Research(C)(16K05258).

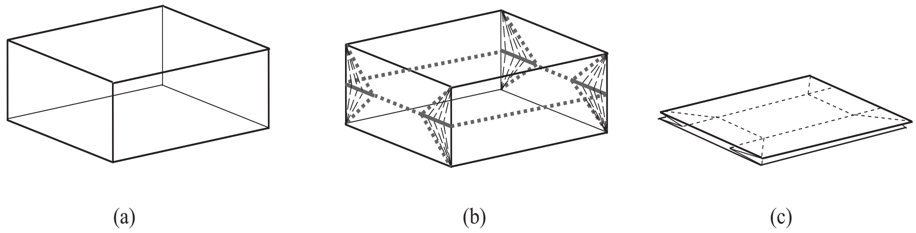

Fig. 1. (a) A box. (b) Mountain and valley creases are shown by bold segments and bold dotted segments respectively for the final flat folded state, together with dashed segments for moving creases. (c) The final flat folded state.

volume (from nonzero to zero), so some faces cannot be rigid, e.g., by changing their shapes continuously by infinitely moving/rolling creases.

Continuous flattenings are known for all convex polyhedra. J.-i. Itoh, C. Nara, and C. Vîlcu [8] gave a method using the cut locus and Alexandrov gluing theorem. The authors et al. [1] showed a surprisingly simple method using the straight skeleton gluing. But it remains an open problem to find continuous flattening motions for nonconvex polyhedra.

Our results. Our main result is the continuous flattening of orthogonal polyhedra (not necessary convex or genus zero); see Fig. 2(a). A polyhedron is called *orthogonal* if the dihedral angle of each edge is $\pm 90°$ (see [6]). By an appropriate choice of x, y, z axes for Euclidean space, we can equivalently define a polyhedron to be orthogonal if every face is orthogonal to the x, y, or z axis.

Theorem 1. *Every orthogonal polyhedron in $\mathbb{R}^3$ can be continuously folded flat so that all faces orthogonal to the z axis remain rigid and translated along the z axis throughout the motion.*

More generally, call a polyhedron *semi-orthogonal* if every face is orthogonal to the z axis or the xy plane; see Fig. 2(b). Any orthogonal polyhedron also satisfies this definition because being orthogonal to the x or y axis implies being orthogonal to the xy plane. We prove more generally that semi-orthogonal polyhedra have flat folding motions:

Theorem 2. *Every semi-orthogonal polyhedron in $\mathbb{R}^3$ can be continuously flat folded such that all faces orthogonal to the z axis remain rigid and translated along the z axis throughout the motion.*

2 Zig-Zag Belts and the Rhombus Property

Before we prove the two theorems, we need some tools for constructing continuous folding motions. We denote by uv the line segment joining points u and v.

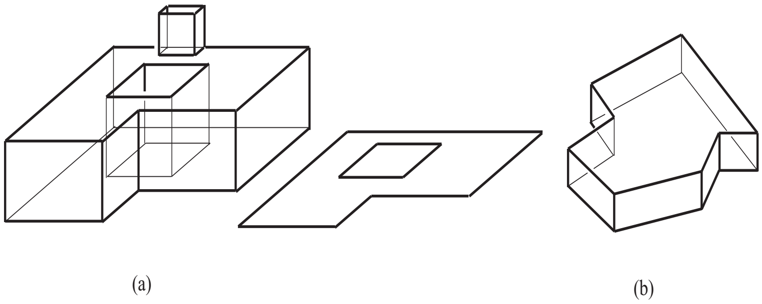

Fig. 2. (a) An example $\mathcal{P}$ of an orthogonal polyhedron with the figure of the base floor of $\mathcal{P}$. (b) An example of a "semi-orthogonal" polyhedron.

Rhombus property. A rhombus $R = abcd$ is a convex quadrilateral with sides of equal length. Rhombi have a very special property useful for flattening a polyhedron, as proposed in [7] and extended to the kite property in [9]. Denote the center of R by h and choose any point q on bh. Consider folding $\triangle acd$ into halves by a valley crease on hd, and folding $\triangle abc$ by a mountain crease on hq and valley creases on aq, cq and qb; see Fig. 3(a). The resulting figure is flexible; see Fig. 3(b, c). Furthermore, if we choose the distances of the two pairs $\{a, c\}$ and $\{b, d\}$ in the resulting 3D figure, such that these distances are not greater than the 2D lengths ac and cd respectively, then there exists a unique point q on hd and unique folding such that the resulting figure satisfies those distances. We call this property the *rhombus property*; see [7, 9] for details.

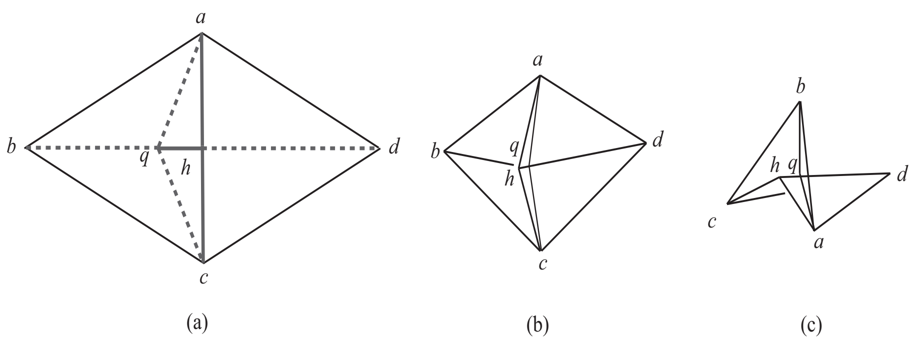

Fig. 3. The rhombus property: (a) a rhombus with mountain creases (grey bold line segments) and valley creases (grey bold dotted line segments); (b) the resulting figure; (c) a view of the resulting figure from a different direction.

Zig-zag belts. Define a *zig-zag belt* B to be a finite orthogonal extrusion in z of a polygonal line lying in a plane parallel to the xy plane; see Fig. 4(a). Equivalently, we can think of a zig-zag belt as a 3D folded state B of a rectangle $T = efvu$ along creases $E_1, E_2, \ldots, E_{n-1}$ parallel (and congruent) to the opposite sides $E_0 = ef$ and $E_n = uv$. We require all E_i's to be parallel to the z axis, and none of the sides to intersect each other, except that we allow E_0 and E_n to overlap, in which case we call the belt *closed*. Call ef and uv the *end sides* of B, and call the line segments in B corresponding to eu and fv the *zig-zag sides* of B. (Either zig-zag side could be the polygonal line that was extruded to form B.) Define the *width* of the belt to be the common length of the E_i's.

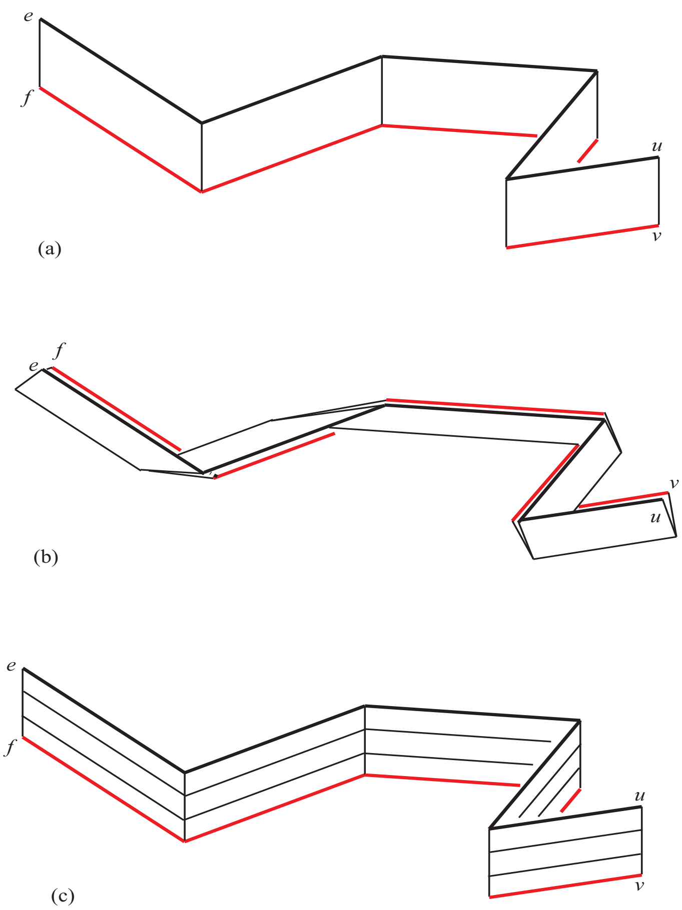

Fig. 4. (a) A zig-zag belt; (b) the flat folded zig-zag belt; (c) zig-zag belts with small widths.

We show how to continuously flatten zig-zag belts into a flat folded state where the zig-zag sides overlap each other; see Fig. 4(b).

Lemma 1. *Consider a zig-zag belt B, and if B is closed, assume that the number of faces is even. Then B can be continuously flattened so that the two zig-zag sides remain rigid and translate only in z.*

Proof. We will show Lemma 1 assuming that B's width is sufficiently small (less than a quantity to be defined in terms of the geometry of either zig-zag side). Then Lemma 1 follows, by slicing B along many uniformly spaced planes parallel to the xy plane, dividing B into congruent zig-zag belts that are z translations of each other and having arbitrarily small width; see Fig. 4(c). Continuously flattening each of these belts in sequence (or in parallel) proves Lemma 1.

Now assume that the belt's width is sufficiently small. We will show Lemma 1 for $n = 2$. This lets us analyze the local folding behavior of the two faces incident to each edge E_i. By synchronizing all of these parallel folding motions to match on the z offsets of the zig-zag sides, the motions will also be consistent on each face, and we obtain a continuous folding of the entire band B. By setting the width sufficiently small (smaller than half the minimum feature size of either zig-zag side), any self-intersections during the band folding must occur locally between one or two adjacent faces, and thus is prevented by the $n = 2$ case.

Now assume that $n = 2$, with $E_0 = ef$, $E_1 = ac$, and $E_2 = E_n = uv$; see Fig. 5(a). Let b and d be points on B so that the quadrilateral $abcd$ is a rhombus with angle $\angle abc = 180° - \angle eau$; see Fig. 5(b). Fold B by mountain creases on h_1b, ab, and bc, and by valley creases on hd and h_2d, where h, h_1, and h_2 are midpoints of ac, ef, and uv respectively; see Fig. 5(b). If we fold these creases by $\pm 180°$, we obtain the target flat folded belt; see Fig. 5(c).

Now we can define the continuous flattening motion that brings B to this flat folded state. First imagine removing the triangle $\triangle abc$ from B, keeping the remaining part S connected at the points a and c; see Fig. 6(b). Then S can be continuously flattened into the corresponding part of the flat folded belt (see Fig. 6(c)), keeping the two zig-zag sides rigid and translating only in z, simply by folding along the two creases h_1b and hh_2. The distance between a and c decreases to zero, and throughout the motion, the distance between b and d in 3D is not greater than the intrinsic distance between b and d in the original 2D figure. Finally, apply the rhombus property to fold the rhombus $abcd$ continuously, synchronizing the motion to match the motion of S.

To be more precise, we give a concrete continuous map for the case when $\angle eau = 90°$ and the edge length of ac is 2; see Fig. 6(d, e, f) and Fig. 7. Orient so that, before folding, $a = (0, 0, 1)$, $b = (0, -1, 0)$, $c = (0, 0, -1)$, and $d = (-1, 0, 0)$. Move a and c to the origin along the z axis with the same speed. The line segment hd remains in the xy plane and translates in the $-y$ direction, and the point b_t remains in the xy plane and translates in the $+x$ direction. Precisely, for t with $0 \le t \le 1$, we have

$$a_t = (0, 0, 1 - t), \qquad b_t = (\sqrt{2t - t^2}, -1, 0) = (\alpha, -1, 0),$$
$$c_t = (0, 0, -1 + t), \text{ and } \quad d_t = (-1, -\sqrt{2t - t^2}, 0) = (-1, -\alpha, 0).$$

where $\alpha = \sqrt{2t - t^2}$. Let p_t be the midpoint of b_t and d_t. Then $p_t = ((\alpha - 1)/2, (-1 - \alpha)/2, 0)$. The point q_t corresponding to q in Fig. 3(b, c) is the

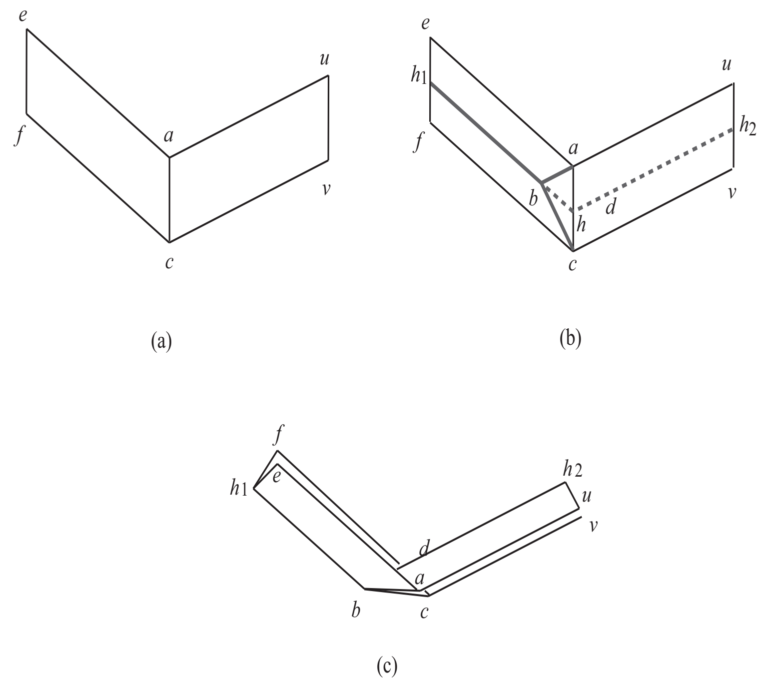

Fig. 5. (a) A zig-zag belt B; (b) B with a crease pattern; (c) the flat folded state of B.

intersection of the plane bisecting $b_t d_t$ and the line segment $h_t d_t$. Because b_t and h_t are on the xy plane, for the sake of simplicity, we omit z coordinates. The line passing through p_t and bisecting $b_t d_t$ is

$$y - (-1 - \alpha)/2 = -\frac{\alpha + 1}{-1 + \alpha}(x - (\alpha - 1)/2).$$

The intersection between this line and the line $y = -\alpha$ is the point q_t. The x coordinate of q_t, denoted x_t, solves to

$$x_t = \frac{\alpha(\alpha - 1)}{\alpha + 1}.$$

As t increases from 0 to 1, α increases from 0 to 1, and hence the absolute value of x_t increases first and then decreases to 0. The maximum absolute value $|x|_{max}$ is attained at $\alpha = \sqrt{2} - 1$, where $|x|_{max} = 3 - 2\sqrt{2}$. Therefore, the area of moving creases is $3 - 2\sqrt{2}$, where the width of the belt is 2.

When $\angle eau \neq 90°$, by using oblique coordinates, we can calculate similarly, however it is a little tedious, so we omit the details.

This motion requires the two edges of a zig-zag side of B to be folded in opposite directions relative to the xy projections of the middle lines. Thus we require a global alternation of fold directions along the zig-zag. If B is closed, the

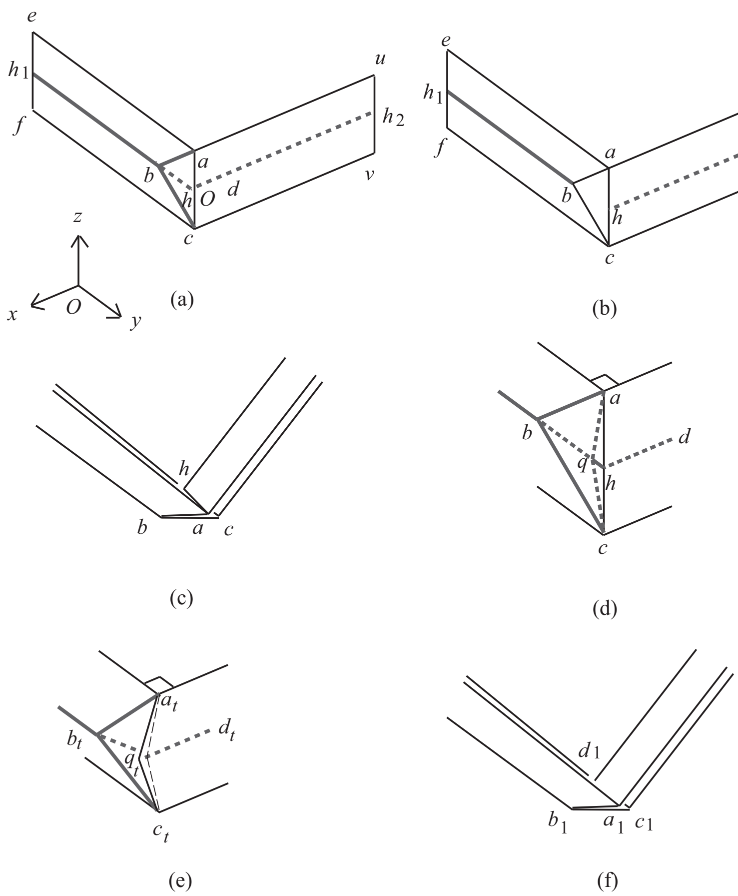

Fig. 6. (a) A zig-zag belt B with crease pattern for the flat folded state. (b) The remaining part S of B. (c) The flat folded state of S. (d) The crease pattern of the rhombus *abcd* for some t, $0 < t < 1$. (e) The figure corresponding to the crease pattern shown in (d). (f) The flat folded state of R.

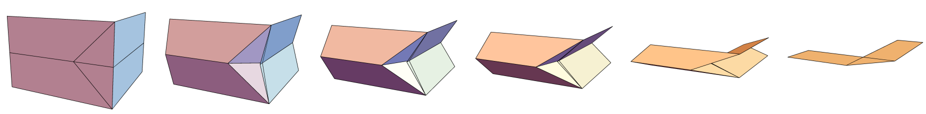

Fig. 7. Continuous flattening animation of the orthogonal corner from Lemma 1, produced with Mathematica.

number of faces is even by assumption, and hence we can continuously flatten B as required. □

3 Continuous Flattening of Orthogonal Polyhedra

It is now relatively easy to continuously flatten orthogonal polyhedra:

Proof (of Theorem 1). Let $\mathcal{P}$ be an orthogonal polyhedron in $\mathbb{R}^3$. Conceptually remove all faces orthogonal to the z axis, and divide the resulting set of faces by planes orthogonal to the z axis that pass through each vertex of $\mathcal{P}$. The result is a collection of zig-zag belts B_i, for $1 \leq i \leq n$, where each belt is closed. Because $\mathcal{P}$ is an orthogonal polyhedron, each belt B_i has an even number of faces. By Lemma 1, each belt B_i can be continuously flattened so that its zig-zag sides remain rigid and translate only in the z direction. Composing these motions sequentially or in parallel, and re-attaching the faces orthogonal to the z axis to the zig-zag sides, we obtain a continuous flattening of $\mathcal{P}$ where the faces orthogonal to the z axis remain rigid and translate only in z. □

4 Continuous Flattening of Semi-Orthogonal Polyhedra

For semi-orthogonal polyhedra, we need to show how to continuously flatten a closed zig-zag belt with an odd number of faces.

Lemma 2. *A zig-zag belt B with two faces and sufficiently small width can be continuously flattened so that the two zig-zag sides remain rigid and translate only along z, and moreover, the zig-zag sides are folded to the same direction of the xy projection of the middle line segments.*

Proof. We use the same notations for points e, f, u, v, a, b, c, d, and h as the proof of Lemma 1, where $\angle abc = \angle adc = 180° - \angle eau$ and the quadrilateral $abcd$ is a rhombus. We move the points b and d toward the convex side of the angle formed by the zig-zag sides. Fold B with mountain creases on bh and valley creases on ab, bc, and hd. Then we obtain a flat folded state that satisfies all requirements; see Fig. 8(a, b).

Consider folding each face of B into halves with valley creases on the middle line segments. Then these faces will intersect each other. The intersection point of the two middle line segments is q_t; see Fig. 8(c, d). Thus the intersection gets resolved by the rhombus $abcd$. In this case, both the distance between a and b, and the distance between b and d, decrease to zero. □

Proof (of Theorem 2). If the number of faces of B is odd, fold one corner by the method proposed in Lemma 2, and fold the other corners by the method proposed in Lemma 1. Then we obtain a continuous motion that satisfies all required conditions. □

References

1. Z. Abel, E. D. Demaine, M. L. Demaine, J.-i. Itoh, A. Lubiw, C. Nara, J. O'Rourke, Continuously flattening polyhedra using straight skeletons. In *Proc. 30th Annual Symposium on Computational Geometry (SoCG)*, 2014. pp. 396–405.

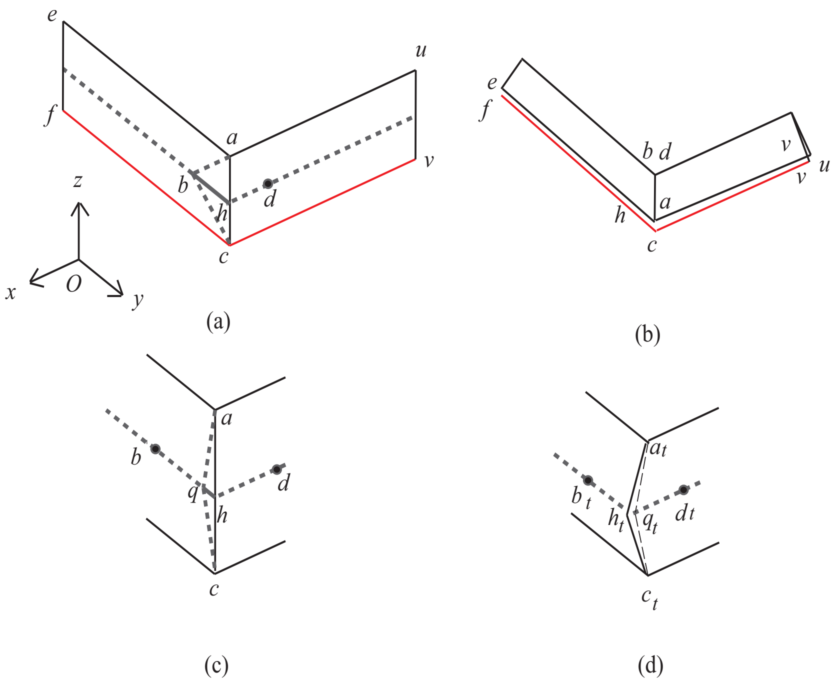

Fig. 8. (a) A zig-zag belt B with crease pattern for a flat folded state. (b) The resulting flat folded state of B. (c) The crease pattern of the rhombus *abcd* for some t, $0 < t < 1$. (d) The resulting 3D figure.

2. M. Bern and B. Hayes. Origami embedding of piecewise-linear two-manifolds. *Algorithmica*, 59(1):3–15, 2011.
3. A. Cauchy, Sur les polygones et les polyèdres. *J. Ecole Polytech.* 9(87):113–148, 1813.
4. R. Connelly, I. Sabitov, A. Walz, The bellows conjecture. *Beiträge Algebra Geom.*, 38:1–10, 1997.
5. E. D. Demaine, M. L. Demaine, and A. Lubiw, Flattening polyhedra. Unpublished manuscript, 2001.
6. E. D. Demaine and J. O'Rourke, *Geometric Folding Algorithms: Linkages, Origami, Polyhedra*, Cambridge University Press, 2007.
7. J.-i. Itoh and C. Nara, Continuous flattening of Platonic polyhedra. In J. Akiyama, J. Bao, M. Kano and X. Tan (eds.), *Proc. Computational Geometry, Graphs and Applications (CGGA 2010)*, LNCS, vol. 7033, pp. 108–121. Springer, 2011.
8. J.-i. Itoh, C. Nara, and C. Vîlcu, Continuous flattening of convex polyhedra. In *Revised Papers, 16th Spanish Meeting on Computational Geometry (EGC 2011)*, LNCS, vol. 7579, pp. 85–97. Springer, 2012.
9. C. Nara, Continuous flattening of some pyramids. *Elem. Math.* 69(2):45–56 (2014).